

RESEARCH

Open Access



Circulating bile acid profiles characteristics and the potential predictive role in clear cell renal cell carcinoma progression

Qi-Chao Wang^{1,2†}, Jing-Yi Cao^{2†}, Guang-Yue Wang^{2†}, Heng Wang¹, Hua Peng², Qian Wang², Zhi-Xiang Yin¹, Jie-Zhou², Ping-An Chang³, Gui-Hua Zhang⁴, Wen-Tao Yao⁵, Jia-Cheng Wu¹ and Chang-Song Pei^{1*}

Abstract

Background The incidence of clear cell renal cell carcinoma (ccRCC) has steadily increased over the past decade, and recent studies have linked bile acid (BA) metabolism to its development. However, the metabolic profile of BAs and their potential as biomarkers in ccRCC pathogenesis remain poorly characterized, making their evaluation crucial for advancing disease understanding and management.

Methods A total of 68 newly diagnosed ccRCC patients and 63 healthy controls were enrolled. Serum bile acid (BA) profiles were measured using Ultra Performance Liquid Chromatography-Tandem Mass Spectrometry (UPLC-MS/MS). The Orthogonal Projections to Latent Structures Discriminant Analysis (OPLS-DA) model analyzed differences in serum BA profiles between ccRCC patients and controls. Additionally, the relationship between BA profiles and tumor heterogeneity parameters was investigated. Receiver Operating Characteristic (ROC) analysis identified potential biomarkers for ccRCC pathogenesis.

Results The BA profile was altered in ccRCC patients and was not influenced by sex or age. Specifically, primary and secondary unconjugated BA fractions were significantly higher in the ccRCC population. Five BA metabolite candidates exhibited the most significant differences between ccRCC patients and controls. Deoxycholic acid (DCA) was associated with pathological pTNM stage classification and grade. Chenodeoxycholic acid (CDCA) and lithocholic acid (LCA), combined with testosterone, showed potential as biomarkers for the pathogenesis of ccRCC.

Conclusion Alterations in the serum BA profile are observed in ccRCC. Deoxycholic acid (DCA) correlates with pathological pTNM stage classification and tumor grade. Additionally, CDCA combined with LCA show potential as biomarkers for ccRCC pathogenesis.

Clinical trial number Not applicable.

Keywords Clear cell renal cell carcinoma, Serum, Bile acid, Biomarker, UPLC-MS/MS

[†]Qi-Chao Wang, Jing-Yi Cao and Guang-Yue Wang contributed equally to this work and share the first authorship.

*Correspondence:
Chang-Song Pei
peichangsong123@126.com

¹Department of Urology, The First Affiliated Hospital of Soochow University, Suzhou, China

²Department of Urology, Xuzhou Cancer Hospital, Affiliated Hospital of Jiangsu University, Xuzhou, China

³Department of Urology, Dongtai People Hospital, Yancheng, China

⁴Department of Hematology, Xuzhou Cancer Hospital, Affiliated Hospital of Jiangsu University, Xuzhou, China

⁵Department of Urology, Suzhou TCM Hospital Affiliated to Nanjing University of Chinese Medicine, Suzhou, China



Introduction

Renal cell carcinoma (RCC) is characterized by high aggressiveness, significant histological subtypes, and mutational heterogeneity [1]. Among these, clear cell renal cell carcinoma (ccRCC) is the predominant pathological type, accounting for approximately 70–80% of all RCC cases [2]. The clinical presentation of ccRCC is often insidious, lacking effective tumor markers and showing resistance to radiotherapy and chemotherapy, making early diagnosis challenging [3]. Clinically, accurately diagnosing small ccRCC tumors and distinguishing RCC from benign renal lesions is difficult [4]. Serum is widely used in biomarker research for various diseases. However, metabolomics and lipidomics studies focusing on distinguishing ccRCC from benign tumors remain scarce, highlighting a significant area for potential diagnostic advancements in ccRCC.

The distinctive pathological feature of ccRCC is the accumulation of large lipid droplets within tumor cells, characterized by the presence of cholesterol esters, which is positively correlated with tumor development [5, 6]. The “clear” cytoplasm of ccRCC cells reflects the presence of these intracellular lipid droplets, which store neutral lipids including cholesterol, cholesterol esters, and triglycerides [7]. Studies indicate that ccRCC cells are heavily reliant on the formation of these lipid droplets for growth and survival, and inhibiting their formation results in cell death [8]. Although the exact mechanisms are not fully understood, cholesterol is the most abundant lipid in ccRCC lipid droplets, playing a crucial role in maintaining cellular homeostasis [9]. Dysregulated lipid metabolism in ccRCC has been implicated in disease progression.

Cholesterol plays multiple critical roles within cells, particularly in cancer cells, and serves as a precursor for bile acids (BAs) [10]. BAs are primarily synthesized in the liver and conjugated with taurine or glycine to form bile salts. These bile salts are released from the gallbladder into the duodenum, where they facilitate the emulsification and absorption of dietary fats, the excretion of excess cholesterol, and the maintenance of gut microbial homeostasis [11]. Previous research has predominantly focused on hepatic and gastrointestinal diseases, with limited studies on renal diseases. Recent studies have highlighted the importance of BA metabolism in ccRCC [7]. Elevated expression of genes in the BA biosynthetic pathway has been observed in ccRCC tumors compared to normal kidney tissue, suggesting a crucial role in ccRCC initiation and progression [11]. Additionally, BA receptors such as the farnesoid X receptor (FXR) and Takeda G protein-coupled receptor 5 (TGR5) are differentially expressed in renal tissues [12, 13]. Cell activity experiments have demonstrated that TGR5 enhances the activity of renal cell carcinoma [14], while FXR was

involved in the growth of renal adenocarcinoma cells [13]. To date, there have been no studies on the changes in serum bile acid composition in ccRCC patients.

This study aims to characterize and compare the absolute concentration and composition of 15 serum BAs in ccRCC patients and control groups to investigate the feasibility of using serum BAs as screening or early warning indicators for ccRCC. Furthermore, we evaluate their correlation with cancer progression characteristics and identify potential biomarkers for the pathogenesis of ccRCC.

Materials and methods

Participants

This investigation encompassed 68 newly diagnosed, untreated ccRCC patients who underwent radical nephrectomy, with no prior targeted therapy or chemotherapy administered. Postoperative pathological examinations confirmed ccRCC in all cases. Serum samples from healthy individuals were included as controls for comparative analysis. All assessments and procedures within the study adhered strictly to the principles outlined in the Declaration of Helsinki regarding human experimentation. The study protocol received approval from the Ethical Committee of the Xuzhou Cancer Hospital (approval no. 2024-02-001-K01), and all participants provided informed written consent after being thoroughly briefed on the study details; consent for publication is not applicable.

Serum collection and biochemical index evaluation

Peripheral venous blood (4–5 ml) was drawn from each participant upon admission, centrifuged at 3500 rpm for 10 min at 4 °C to obtain serum, which was then stored at -80 °C for subsequent analysis. Serum biochemical parameters were analyzed using a Beckman AU5800 automated biochemical analyzer. Information collected included body mass index (BMI) [15], and various biochemical indicators such as aspartate aminotransferase (AST), alanine aminotransferase (ALT), gamma-glutamyl transferase (GGT), alkaline phosphatase (ALP) creatinine, uric acid, and cystatin C. Participant characteristics and clinical parameters are detailed in Table 1.

Serum targeted bile acid profile assessment

BAs were quantified using an Ultrahigh-Performance Liquid Chromatography-Tandem Mass Spectrometry (UPLC-MS/MS) system (Waters Corporation, Milford, Massachusetts, USA) equipped with a triple quadrupole mass spectrometer and a Jet Stream electrospray ionization (ESI) source. Internal standards (ISs) and BAs were obtained from Sigma-Aldrich (Darmstadt, Germany), with abbreviations detailed in the supporting information (Table S1). ISs were prepared by mixing isotope-labeled

Table 1 General characteristics of the CcRCC and control groups

Characteristic	Group	N	Mean	SD	25th	75th	P
Age	Con	63	52.016	13.366	42.500	62.500	0.06
Age	ccRCC	68	56.706	8.205	51.000	63.250	
BMI	Con	63	24.979	3.067	23.100	27.150	0.89
BMI	ccRCC	68	25.289	3.328	23.440	26.670	
AST	Con	63	20.063	5.869	15.500	22.500	0.26
AST	ccRCC	68	21.703	7.768	16.000	23.675	
ALT	Con	63	21.397	12.323	12.000	28.500	0.23
ALT	ccRCC	68	23.401	11.576	13.875	28.300	
GGT	Con	63	39.302	73.202	15.000	28.500	0.25
GGT	ccRCC	68	28.596	17.077	16.450	36.000	
ALP	Con	63	81.857	34.647	69.500	86.000	0.09
ALP	ccRCC	68	73.000	17.428	62.500	82.250	
urea nitrogen	Con	63	5.730	2.430	4.485	6.680	0.76
urea nitrogen	ccRCC	68	5.835	2.708	4.375	6.900	
creatinine	Con	63	72.873	35.240	56.000	77.500	0.44
creatinine	ccRCC	68	76.209	79.113	53.800	76.575	
uric acid	Con	63	299.508	82.631	248.500	333.000	0.10
uric acid	ccRCC	68	320.588	96.895	253.750	382.250	
cystatin C	Con	63	0.932	0.356	0.745	1.000	0.10
cystatin C	ccRCC	68	1.052	0.751	0.790	1.042	

standards in methanol and diluting with deionized water. For serum analysis, 50 μ L of serum was mixed with 5 μ L of IS and 150 μ L of precooled methanol. After centrifugation at 12,000 g for 10 min at 4 $^{\circ}$ C, 50 μ L of the supernatant was combined with 50 μ L of deionized water and transferred to autosampler vials for analysis. Chromatographic separation was performed on an ACQUITY UPLC BEH C18 column (1.7 μ m, 100 mm \times 2.1 mm) at 45 $^{\circ}$ C with a gradient elution: 0–3 min, 35% B; 3–4.5 min, 35–60% B; 4.5–5 min, 65–100% B; 5–6 min, 100–35% B. Mobile phase A was 10 mmol/L ammonium acetate in water, and mobile phase B was 0.1% formic acid in acetonitrile, at a flow rate of 0.4 mL/min. Mass spectrometric detection was conducted in negative ion mode using Multiple Reaction Monitoring (MRM). Nitrogen was used as the nebulizer and cone gas, with source and desolvation temperatures set at 150 $^{\circ}$ C and 450 $^{\circ}$ C, respectively.

Data were analyzed using MassLynx software (Version 4.1), with calibration curves generated by linear regression. The linearity of all bile acids was validated within the range of 1.0–6000.0 nmol/L, with coefficients of determination (R^2) exceeding 0.99 for all compounds. The calibration curves for all measured BAs demonstrated excellent linearity within the defined quantification range, with R^2 values exceeding 0.99 for all compounds. A total of 15 BAs were analyzed, including six primary BAs: cholic acid (CA, $R^2 = 0.999$), chenodeoxycholic acid (CDCA, $R^2 = 0.999$), glycocholic acid (GCA, $R^2 = 0.999$), taurocholic acid (TCA, $R^2 = 0.999$), glycochenodeoxycholic acid (GCDCA, $R^2 = 0.998$), and

taurochenodeoxycholic acid (TCDC, $R^2 = 0.997$); and nine secondary BAs: deoxycholic acid (DCA, $R^2 = 0.996$), ursodeoxycholic acid (UDCA, $R^2 = 0.999$), lithocholic acid (LCA, $R^2 = 0.998$), glycodeoxycholic acid (GDCA, $R^2 = 0.999$), taurodeoxycholic acid (TDCA, $R^2 = 0.999$), glyoursodeoxycholic acid (GUDCA, $R^2 = 0.998$), tauroolithocholic acid (TLCA, $R^2 = 0.999$), glycolithocholic acid (GLCA, $R^2 = 0.998$), and tauroursodeoxycholic acid (TUDCA, $R^2 = 0.997$). These values underscore the accuracy and reliability of the quantification method employed in this study. The limits of quantification (LOQs) for the bile acids ranged from 1.0 to 10.0 nmol/L. Intra- and inter-day precision, expressed as relative standard deviations (RSDs), were below 15%. Additionally, the coefficients of variation (CoVs) for both high and low quality control (QC) samples of the 15 BAs were also below 15%. To ensure the accuracy of quantification and identification, chromatographic peaks were calibrated based on retention times and parameters related to the peak shape of each BA. This calibration enabled reliable comparison of BA concentration differences. Randomly inserted QC samples were included for every 10 serum samples to monitor the reproducibility of instrument performance. The overlap of the total ion chromatograms (TICs) for the QC samples was used as a measure of stability; higher overlap indicated better instrument stability. The final concentrations were calculated by integrating the peak areas and applying the calibration curve equation.

Statistical analysis

Statistical analyses were performed using JASP 19.0, with supplementary analysis in Origin. Bile acid distribution among groups was visualized using SIMCA-P software v14.1 (Umetrics AB, Umea, Sweden). Principal component analysis (PCA) and orthogonal partial least squares-discriminant analysis (OPLS-DA) models were constructed based on the metabolomics data. The variable importance in the projection (VIP) of the first principal component obtained from the OPLS-DA analysis was determined. In the univariate analysis, metabolites with a $VIP > 1.0$ and P -value < 0.05 were considered significantly different. Moreover, the quality of the OPLS-DA model was assessed using standard parameters (R2X and Q2) [16]. Categorical data were analyzed using the chi-square test. For continuous variables, data were expressed as means \pm standard error of the mean (SEM) if normally distributed, or as medians and interquartile ranges if not. Independent sample t -tests were used for normally distributed data meeting parametric assumptions, while the Mann-Whitney U test was used for non-normally distributed data. Regression model to identify independent risk factors for ccRCC, employing forward stepwise regression. A P -value of < 0.05 was considered statistically significant.

Results

Characteristics and analysis of serum bile acid profile in CcRCC patients

Clinical data were collected for sex-matched patients with ccRCC and healthy controls, showing no significant differences in age, BMI, fasting blood glucose, blood pressure, liver and kidney function, total protein, albumin, or cystatin C (Table 1). Both primary and secondary unconjugated BAs were significantly higher in ccRCC patients (Fig. 1A). Ratio analysis of the 15 BA metabolites to total BAs indicated relatively higher percentages of LCA and DCA, and lower percentages of TLCA and GCDCA in ccRCC patients (Fig. 1B). Regarding the distribution of BA levels, we have provided bar plots of BA concentrations for control and ccRCC groups to facilitate visualization of the data distribution (Fig. 1C). These distributions clearly highlight variations in individual BA levels between the two groups, emphasizing the differences observed in our study. Serum BA level analysis revealed significantly elevated concentrations of free BAs (CA, CDCA, DCA, UDCA) and conjugated BAs (GDCA, GLCA) in the ccRCC group compared to controls (Table S2).

Since strong significant differences were found in the BAs, to better quantify the difference between the ccRCC and control group, besides frequentist statistics, Bayesian T-test was used to compare the difference between the DCA and CA of ccRCC group and Control group. As

shown in Fig. 2, A Bayes factor of 158 suggests that an alternative model is 158 times more favored than a null model, given the data.

Identification of significantly different BAs associated with CcRCC

To comprehensively compare the BA metabolomic profiles between ccRCC patients and controls, we employed the PCA and OPLS-DA model to assess the degree of diversity. The PCA model demonstrated an inability to distinctly separate the two groups (R2X(cum) 0.454, Q2(cum) 0.095; Fig. 3A). The OPLS-DA model revealed a clear distinction between the ccRCC and Control groups, with serum BA profiles clustering into two distinct groups, indicating significant differences. The OPLS-DA model exhibited clearer discrimination, though not entirely conclusive (R2X(cum)=0.728, Q2(cum)=0.141; Fig. 3B). Considering the inherent variability in human biological samples [16, 17], the R2X value being above 0.5 (with a relatively low Q2 value of at 0.141) was deemed acceptable. The analysis identified four BAs—DCA, CA and CDCA—with VIP values greater than 1, showing significant differences ($P < 0.05$) in the univariate analysis between the groups (Fig. 3C, Table S2). To further validate the prediction model, we conducted permutation tests. The Q2 intercept value falling below 0 indicated a reliable and non-overfitted model (Fig. 3D). Notably, DCA exhibited the most significant elevation in the ccRCC group and held substantial relevance in the BA composition compared to controls (VIP score=3.24771, $P < 0.001$).

The candidate value of BAs in serum for CcRCC

Our objective was to ascertain the predictive utility of BAs for ccRCC. We performed receiver operating characteristic (ROC) and logistic regression analyses on the differential serum BAs identified. ROC curves distinguished healthy controls from ccRCC patients, evaluating the area under the curve (AUC), and determining the sensitivity and specificity of cut-off values for each BA (Fig. 4A-B; Table 2). Serum DCA exhibited the highest correlation with ccRCC, yielding an AUC of 0.82 ($P < 0.001$). The sensitivity and specificity for predicting ccRCC were 61.8% and 81.0%, respectively. Subsequent logistic regression combined with ROC analysis, encompassing DCA, TCDCA, LCA, TLCA, further enhanced the predictive performance for ccRCC. The combined model yielded an AUC of 0.847, with a sensitivity of 67.6% and specificity of 84.1%, highlighting the potential of BA concentration measurement, particularly conjugated BAs, in ccRCC screening. Additionally, we performed a multivariate logistic regression analysis; the results indicated that while there was no significant effect

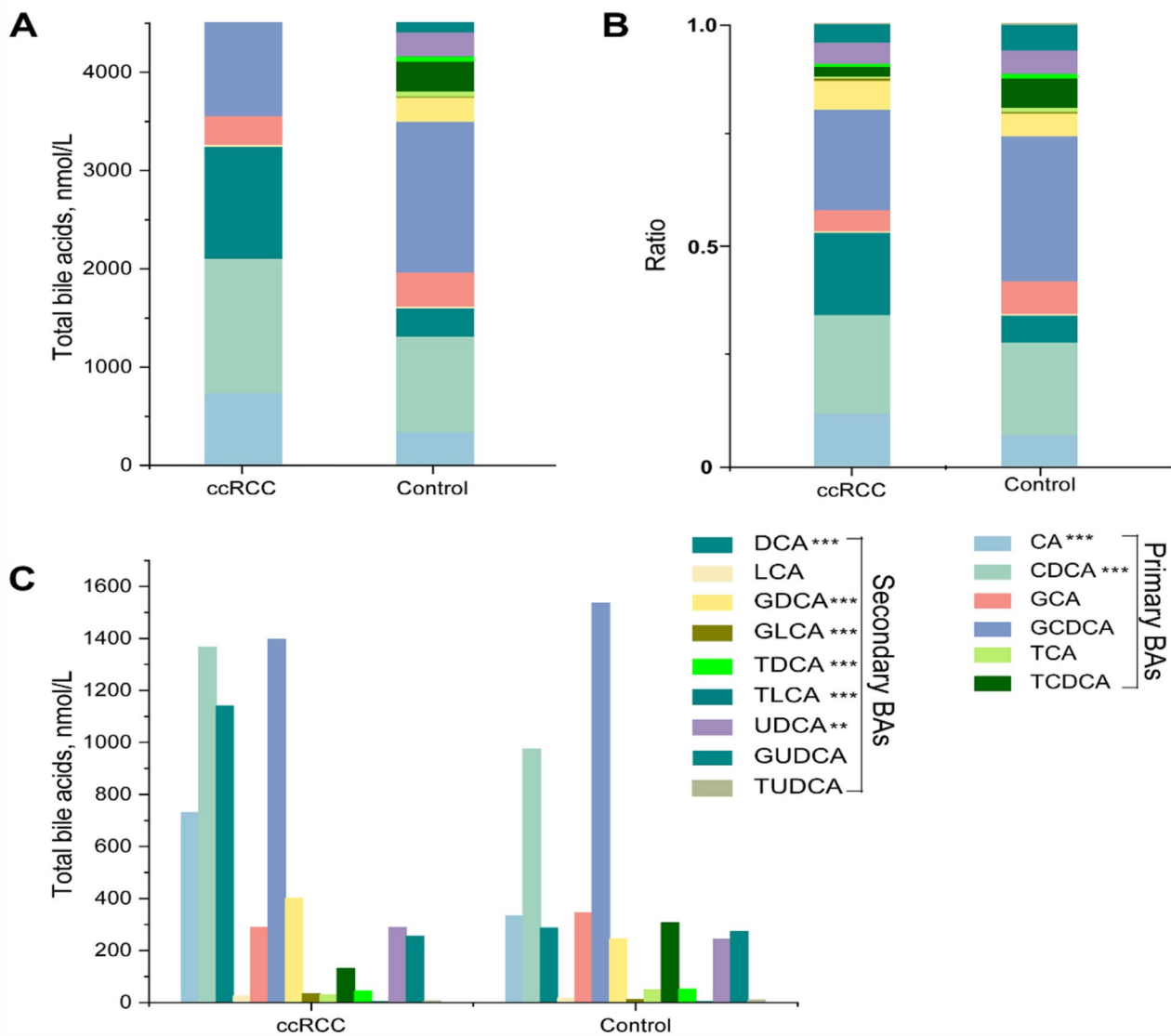


Fig. 1 Comparison of serum BA pools between the ccRCC and Control groups. **(A)** Serum BA composition of total BAs, including unconjugated and conjugated forms, in the ccRCC and Control groups. **(B)** Relative fractions of BAs as proportions in the ccRCC and Control groups (The proportions of BA species were calculated as concentrations of BA species / Total BA × 100%). **(C)** Bar plots of BA concentrations for control and ccRCC groups. * $P < 0.05$, ** $P < 0.01$, *** $P < 0.001$

of sex on the BA profiles, age may have an influence, as suggested by a near-significant difference (Table S4).

Discussion

ccRCC is the most prevalent and deadly subtype of renal cancer, accounting for 70–80% of cases [18]. Its high mortality rate is primarily due to its asymptomatic early stages, resulting in late diagnosis for about 30% of patients. Currently, invasive biopsy is the only definitive diagnostic method, as no specific clinical biomarkers are available for ccRCC [3]. Therefore, developing early diagnostic methods is crucial. Recent research into the metabolic pathways of ccRCC cells offers promising avenues for non-invasive and accurate screening technologies,

which could significantly enhance diagnosis and treatment strategies [19, 20]. ccRCC is a metabolic disease marked by significant alterations in cellular metabolism, including changes in glycolysis, mitochondrial bioenergetics, oxidative phosphorylation (OxPhos), and lipid metabolism [21, 22]. Morphologically, ccRCC cells are characterized by an accumulation of lipids and glycogen, reflecting these metabolic reprogramming processes.

Recent studies have underscored the crucial role of BAs in regulating key metabolic pathways, including glycolysis, mitochondrial function, and lipid metabolism—processes central to RCC pathogenesis. Alterations in BA metabolism are linked to shifts in cellular energy production and lipid homeostasis, reinforcing the metabolic

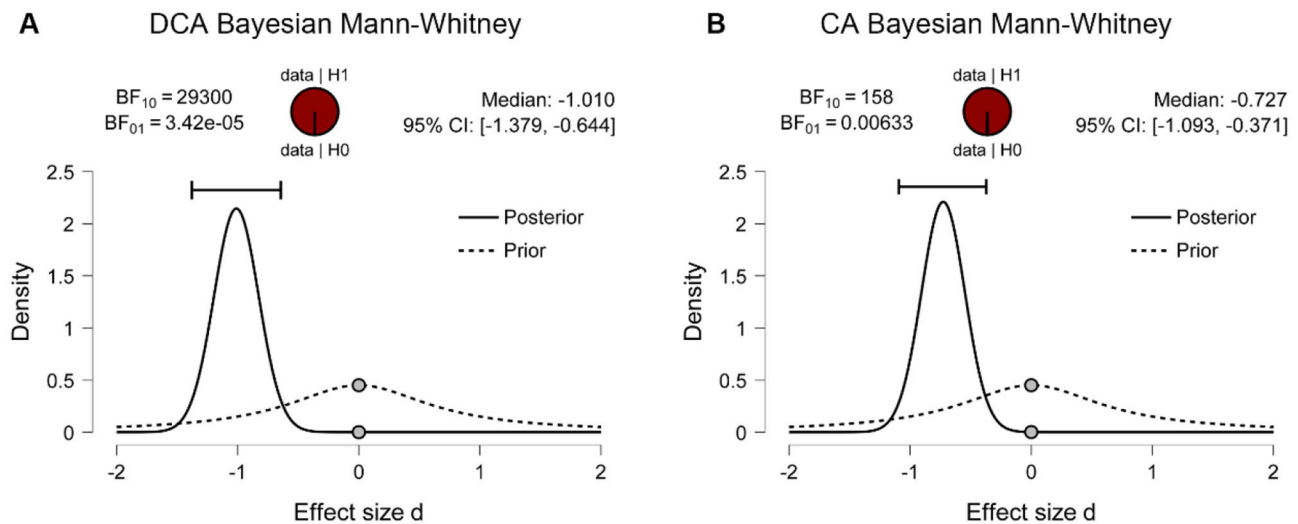


Fig. 2 Bayesian Independent Samples T-Test for ccRCC Patients and Controls (**A**). DCA Bayesian Mann-Whitney. (**B**) CA Bayesian Mann-Whitney. The probability wheel on top visualizes the evidence that the data provide for the two rival hypotheses. The two gray dots indicate the prior and posterior density at the test value. The median and the 95% central credible interval of the posterior distribution are shown in the top right corner. $BF_{10} = 29300$ means very strong evidence support the alternative hypothesis. Note: Following the proposals made by Wetzels, van Ravenzwaaij, and Wagenmakers (2015), based on Jeffreys (1961), the Bayesian findings were interpreted as follows. (I) Clear evidence for the alternate hypothesis (extremely strong evidence: $BF_{10} > 100$; very strong evidence: 30–100; strong evidence: 10–30; moderate evidence: 3–10). (II) Anecdotal evidence for the alternate hypothesis: $BF_{10} = 1-3$; (III) No evidence: $BF_{10} = 1$

reprogramming characteristic of RCC [23]. These findings suggest that BAs may serve as both critical regulators of RCC metabolism and potential biomarkers for disease progression. Consequently, ccRCC exemplifies the role of metabolic reprogramming in cancer, highlighting the importance of metabolic shifts in its pathogenesis [24, 25]. Additionally, cholesterol, a key component in cancer cell physiology and a precursor for BAs, is vital for various cellular functions, further linking lipid metabolism with tumor progression. BAs are synthesized in the liver, conjugated with taurine or glycine to form bile salts, and stored in the gallbladder [26]. Upon release into the duodenum, these bile salts facilitate the emulsification and absorption of dietary fats, promote the excretion of excess cholesterol, and help maintain gut microbial homeostasis [27]. These processes are crucial for sustaining metabolic health and have significant implications in oncological contexts. BAs play roles in various cancers, synthesized in the liver but involving multiple organs for balance and excretion. Initially recognized as carcinogenic due to their signaling roles [28, 29], recent studies suggest anti-tumor properties in some cancers, such as breast cancer [30, 31]. The serum BA profile reflects the bile profile, making it feasible to use serum BAs as screening markers for ccRCC. However, few studies have focused on using serum BAs to distinguish ccRCC from benign tumors, which would significantly aid in differential diagnosis. Our study revealed significant alterations in the serum bile acid profile of ccRCC patients, identifying four free BAs (DCA, CDCA, UDCA) and two conjugated bile acids (GDCA, GLCA) with statistically

significant differences. Among these, DCA was the most discriminative factor between groups. Additionally, DCA demonstrated the highest diagnostic efficacy as a single marker, with an AUC of 0.82.

DCA, primarily produced in the cecum and proximal colon by microbial activity, exhibits both antibacterial properties and toxicity [32]. DCA acts as a tumor-promoting agent by inducing apoptosis and promoting cancer cell proliferation, significantly contributing to various cancers. DCA induced oxidative stress, DNA damage, and inflammation, leading to esophageal adenocarcinoma (EAC), while UDCA mitigated DCA-induced injury [33, 34]. Acidic bile salts activated telomerase via a c-Myc-dependent pathway, and DCA induced a metastatic phenotype in gastric cancer cells [35, 36]. Additionally, hydrophobic BAs like DCA were prominent promoters of liver cancer, contributing to hepatocellular carcinoma (HCC) [37, 38]. The Western diet's tumor-promoting activity was linked to elevated colonic BA concentrations, mainly LCA and DCA, as observed in colorectal carcinoma (CRC) patients [39]. Notably, low concentrations of DCA (0.05–0.3 mM) inhibited colonic cell proliferation through cell cycle arrest and apoptosis pathways [40]. DCA also modulated the expression of breast cancer type 1 susceptibility protein (BRCA1) and the estrogen receptor, influencing the drug sensitivity of ovarian cancer cells [41].

BAs play a crucial role in kidney pathophysiology through the activation of the farnesoid X.

receptor (FXR) and G protein-coupled bile acid receptor 1 (GPBAR1/TGR5) [42]. These receptors have been

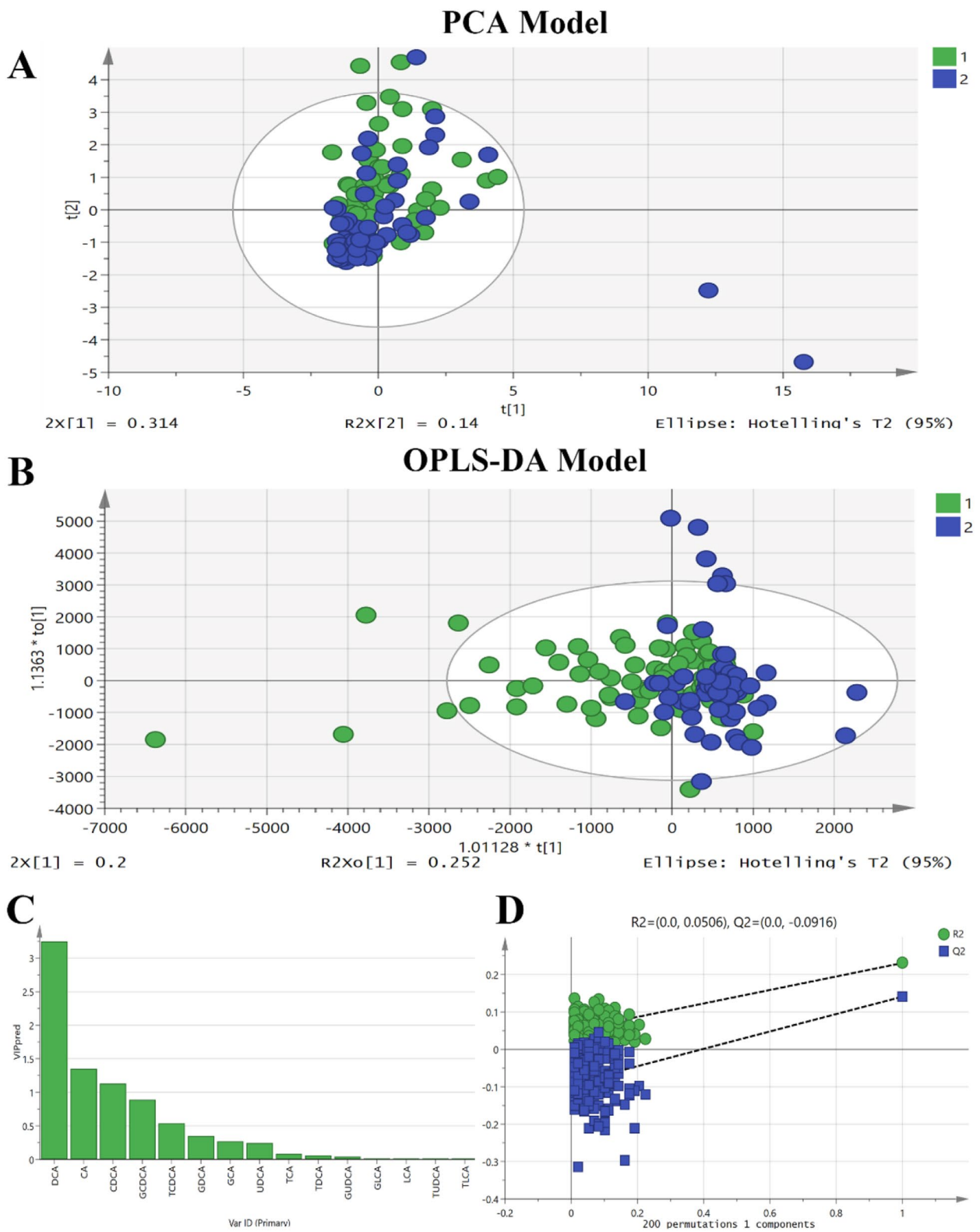


Fig. 3 (See legend on next page.)

(See figure on previous page.)

Fig. 3 PCA model and OPLS-DA model plots derived from BA metabolomic profiles comparing ccRCC and Control groups. **(A)** Serum BA profiles displayed in Principal component analysis (PCA) model scores plot for ccRCC group (green) and Control group (blue). **(B)** Serum BA profiles displayed in OPLS-DA scores plot for ccRCC group (green) and Control group (blue). **(C)** VIP scores from OPLS-DA highlighting significant serum BA profile differences between the ccRCC and Control groups (VIP value > 1 indicates discrimination importance). **(D)** Permutation test of OPLS-DA Model of the BAs. The permutation plot strongly indicates that the model is valid. The criteria for validity are: (1) All blue Q2-value to the left are lower than the original points to the right; (2) The blue regression line of the Q2-points intersects the vertical axis (on the left) at, or below zero

implicated in RCC pathogenesis. TGR5 was reported to inhibit inflammation via the NF- κ B pathway, mitigating diabetic nephropathy and potentially preventing RCC cell proliferation [43, 44]. FXR, essential for cholesterol/BA homeostasis, stimulated renal adenocarcinoma proliferation; its knockdown suppressed tumor growth without harming normal cells [13]. TCGA data revealed dysregulated TGR5 and FXR in RCC tissues, highlighting their significance [45]. DCA, a potent TGR5 and FXR agonist, inhibited acetylcholine-induced inositol phosphate formation, likely targeting inositol polyphosphate hydrolase, whose activity was reduced in renal tumors [46]. Elevated DCA conjugates in RCC patients inhibited this enzyme's activity, contributing to cancer progression. Based on the analysis of BA profiles in (ccRCC, we identified potential BA biomarkers for ccRCC pathogenesis. Our findings indicated that the combined use of DCA, LCA, TCDCA and TLCA provided a more effective predictive model for ccRCC than DCA alone. These results enhance our understanding of BA-related signaling pathways, suggesting that future research should investigate downstream molecules within these pathways to further elucidate their roles in ccRCC.

Our study highlights the altered BA profile in the serum of ccRCC patients, revealing significant changes in the circulating levels of various bile acids. Interestingly, while our study focuses on the circulating bile acid profile in serum, Li et al. [47], reported a decrease in bile acid levels within ccRCC tumor tissues, despite an increase in cholesterol. This apparent discrepancy may arise from differences in the biological compartments analyzed. In our study, the serum BA levels reflect systemic metabolic changes, influenced by factors such as liver function, bile acid synthesis, and intestinal absorption. In contrast, tumor tissues are known to undergo metabolic reprogramming, which may lead to localized alterations in bile acid metabolism, including reduced BA levels in the tumor microenvironment. These differences underscore the complexity of metabolic shifts in ccRCC and highlight the need for further studies that directly compare bile acid levels in both serum and tumor tissue to better understand their role in disease progression. This discrepancy between serum and tumor tissue may also be attributed to the unique properties of the tumor microenvironment. Tumors often exhibit altered lipid and energy metabolism, which may affect the local synthesis, transport, and catabolism of bile acids. Additionally,

the interaction between tumor cells and the surrounding stromal cells can influence the uptake and secretion of BAs. These factors suggest that while serum BAs may serve as potential biomarkers of systemic disease, their role in the local tumor environment might differ, and further research is needed to explore these dynamics in greater detail.

Our study has several limitations that warrant a cautious interpretation of our findings. The single-center, retrospective, and cross-sectional design inherently limits the generalizability of our results and precludes establishing a causal relationship between altered bile acid (BA) profiles and the development of clear cell renal cell carcinoma (ccRCC). Although our findings indicate that deoxycholic acid (DCA) is correlated with pathological grade, stage, and related clinical indicators, the study design does not allow us to determine whether these alterations in DCA levels are a contributing factor to tumor progression or simply a reflection of underlying metabolic changes associated with ccRCC. Additionally, selection bias and the limited sample size, particularly the absence of late-stage ccRCC cases, may have affected the identification of independent risk factors and restricted the statistical power necessary for robust subgroup analyses. For instance, there is a near-significant age difference between ccRCC patients and controls ($P=0.06$), and to address this, we performed a multivariate logistic regression analysis including both age and sex as covariates. The results indicated that while sex did not have a significant effect on BA profiles, age may have a near-significant effect, suggesting that the observed age influence might be attributable to the sample limitations inherent in our study design. Moreover, our study did not examine the interplay between BAs and gut microbiota—a relationship increasingly recognized as crucial in metabolic regulation, as the gut-liver axis plays a significant role in BA metabolism and alterations in the gut microbiome could impact BA synthesis, transformation, and systemic circulation. Future studies integrating microbiome analysis, as well as multicenter prospective randomized controlled trials with larger cohorts, will be critical to validate our findings and to develop potential BA-based diagnostic and therapeutic strategies for ccRCC.

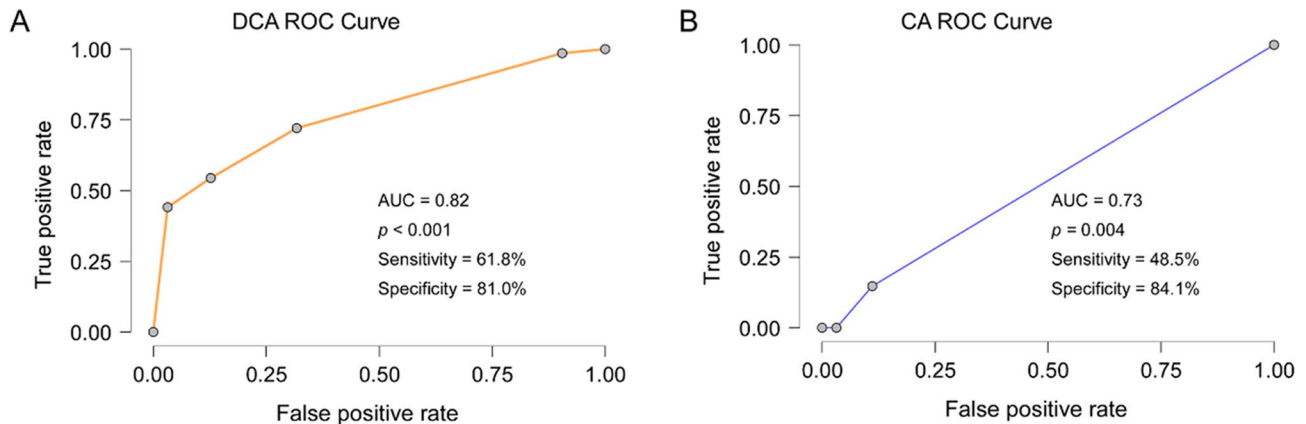


Fig. 4 ROC curve analysis of predictive value of DCA and CA indicators for ccRCC patients. **(A)** ROC curve for DCA in predicting ccRCC patients. **(B)** ROC curve for CA in predicting ccRCC patients. In this study, the ROC curves was analyzed by logistic regression part of JASP [JASP Team (2024). JASP (Version 0.19.2)]

Table 2 The model summary of the logistic regression

Model	AIC	BIC	df	ΔX^2	p	McFadden R^2	Nagelkerke R^2	Tjur R^2
M_0	183.414	186.289	130			0.000		0.000
M_1	131.457	145.833	126	59.957	< 0.001	0.330	0.490	0.374

Supplementary Information

The online version contains supplementary material available at <https://doi.org/10.1186/s12882-025-04142-y>.

Supplementary Material 1

Acknowledgements

The authors would like to thank the Xuzhou City Health Commission and Jiangsu University for their support in this study.

Author contributions

QC W, JY C and GY W contributed equally to this work as co-first authors. QC W, JY C and GY W were responsible for the study design. H W and H P conducted the key experiments and performed data analysis. Q W and Z X Y carried out the clinical investigations. J Z, PA C, GH Z, WT Y and JC W were involved in data collection and manuscript preparation. CS P supervised the overall project and provided critical revision of the manuscript. All authors read and approved the final manuscript.

Funding

This work was supported by the 2023 Xuzhou Municipal Health Commission Science and Technology Youth Projects (Project Number: XWKYHT20230001).

Data availability

The original contributions presented in the study are included in the article/supplementary material, further inquiries can be directed to the corresponding author/s.

Declarations

Ethics approval and consent to participate

The study complied with the basic requirements of the Declaration of Helsinki. And the study protocol received approval from the Ethical Committee of the Xuzhou Cancer Hospital (approval no. 2024-02-001-K01), and all participants provided informed written consent after being thoroughly briefed on the study details.

Consent for publication

This manuscript does not include any identifying images or personal or clinical details of participants that could compromise their anonymity. Therefore, obtaining consent for publication is not applicable.

Competing interests

The authors declare no competing interests.

Received: 14 October 2024 / Accepted: 18 April 2025

Published online: 23 April 2025

References

- Liu W, Ren D, Xiong W, Jin X, Zhu L. A novel FBW7/NFAT1 axis regulates cancer immunity in sunitinib-resistant renal cancer by inducing PD-L1 expression. *J Exp Clin Cancer Res.* 2022;41(1):38.
- Wang L, Yang G, Zhao D, Wang J, Bai Y, Peng Q, Wang H, Fang R, Chen G, Wang Z, et al. CD103-positive CSC exosome promotes EMT of clear cell renal cell carcinoma: role of remote miR-19b-3p. *Mol Cancer.* 2019;18(1):86.
- Hu J, Wang SG, Hou Y, Chen Z, Liu L, Li R, Li N, Zhou L, Yang Y, Wang L, et al. Multi-omic profiling of clear cell renal cell carcinoma identifies metabolic reprogramming associated with disease progression. *Nat Genet.* 2024;56(3):442–57.
- Li X, Shong K, Kim W, Yuan M, Yang H, Sato Y, Kume H, Ogawa S, Turkez H, Shoaie S, et al. Prediction of drug candidates for clear cell renal cell carcinoma using a systems biology-based drug repositioning approach. *EBioMedicine.* 2022;78:103963.
- Riscal R, Bull CJ, Mesaros C, Finan JM, Carens M, Ho ES, Xu JP, Godfrey J, Brennan P, Johansson M, et al. Cholesterol auxotrophy as a targetable vulnerability in clear cell renal cell carcinoma. *Cancer Discov.* 2021;11(12):3106–25.
- Xiao W, Wang C, Chen K, Wang T, Xing J, Zhang X, Wang X. MiR-765 functions as a tumour suppressor and eliminates lipids in clear cell renal cell carcinoma by downregulating PLP2. *EBioMedicine.* 2020;51:102622.
- Riscal R, Gardner SM, Coffey NJ, Carens M, Mesaros C, Xu JP, Xue Y, Davis L, Demczyszyn S, Vogt A, et al. Bile acid metabolism mediates cholesterol homeostasis and promotes tumorigenesis in clear cell renal cell carcinoma. *Cancer Res.* 2024;84(10):1570–82.
- Peng S, Wang Z, Tang P, Wang S, Huang Y, Xie Q, Wang Y, Tan X, Tang T, Yan X, et al. PHF8-GLUL axis in lipid deposition and tumor growth of clear cell renal cell carcinoma. *Sci Adv.* 2023;9(31):eadf3566.

9. Zhang S, Fang T, He Y, Feng W, Yu Z, Zheng Y, Zhang C, Hu S, Liu Z, Liu J, et al. VHL mutation drives human clear cell renal cell carcinoma progression through PI3K/AKT-dependent cholesteryl ester accumulation. *EBioMedicine*. 2024;103:105070.
10. Cong J, Liu P, Han Z, Ying W, Li C, Yang Y, Wang S, Yang J, Cao F, Shen J, et al. Bile acids modified by the intestinal microbiota promote colorectal cancer growth by suppressing CD8(+) T cell effector functions. *Immunity*. 2024;57(4):876–e889811.
11. Jia W, Li Y, Cheung KCP, Zheng X. Bile acid signaling in the regulation of whole body metabolic and immunological homeostasis. *Sci China Life Sci*. 2024;67(5):865–78.
12. Zhao CL, Amin A, Hui Y, Yang D, Cao W. TGR5 expression in normal kidney and renal neoplasms. *Diagn Pathol*. 2018;13(1):22.
13. Fujino T, Sakamaki R, Ito H, Furusato Y, Sakamoto N, Oshima T, Hayakawa M. Farnesoid X receptor regulates the growth of renal adenocarcinoma cells without affecting that of a normal renal cell-derived cell line. *J Toxicol Sci*. 2017;42(3):259–65.
14. Guan Z, Luo L, Liu S, Guan Z, Zhang Q, Wu Z, Tao K. The role of TGR5 as an onco-immunological biomarker in tumor staging and prognosis by encompassing the tumor microenvironment. *Front Oncol*. 2022;12:953091.
15. Matthew LB, Danielle SC, David PM, Daniel LC. Metabolic bariatric surgery, alcohol misuse and liver cirrhosis: a narrative review. *Metabolism Target Organ Damage*. 2024;4(3):29.
16. Yu J, Zhang Y, Zhu Y, Li Y, Lin S, Liu W, Tao T. Circulating bile acid profile characteristics in PCOS patients and the role of bile acids in predicting the pathogenesis of PCOS. *Front Endocrinol (Lausanne)*. 2023;14:1239276.
17. Jiang Y, Qi J, Xue X, Huang R, Zheng J, Liu W, Yin H, Li S. Ceramide subclasses identified as novel lipid biomarker elevated in women with polycystic ovary syndrome: a pilot study employing shotgun lipidomics. *Gynecol Endocrinol*. 2020;36(6):508–12.
18. Moch H, Amin MB, Berney DM, Comperat EM, Gill AJ, Hartmann A, Menon S, Raspollini MR, Rubin MA, Srigley JR, et al. The 2022 world health organization classification of tumours of the urinary system and male genital Organs-Part A: renal, penile, and testicular tumours. *Eur Urol*. 2022;82(5):458–68.
19. Li GX, Chen L, Hsiao Y, Mannan R, Zhang Y, Luo J, Petralia F, Cho H, Hosseini N, Leprevost FDV, et al. Comprehensive proteogenomic characterization of rare kidney tumors. *Cell Rep Med*. 2024;5(5):101547.
20. Simonetta L, Enrica B, Amedeo L. Metabolic primary liver cancer in adults: risk factors and pathogenic mechanisms. *Metabolism Target Organ Damage*. 2023;3(1):5.
21. di Meo NA, Lasorsa F, Rutigliano M, Milella M, Ferro M, Battaglia M, Dittono P, Lucarelli G. The dark side of lipid metabolism in prostate and renal carcinoma: novel insights into molecular diagnostic and biomarker discovery. *Expert Rev Mol Diagn*. 2023;23(4):297–313.
22. di Meo NA, Lasorsa F, Rutigliano M, Loizzo D, Ferro M, Stella A, Bizzoca C, Vincenti L, Pandolfo SD, Autorino R et al. Renal cell carcinoma as a metabolic disease: an update on main pathways, potential biomarkers, and therapeutic targets. *Int J Mol Sci*. 2022;23(22).
23. Bombelli S, Torsello B, De Marco S, Lucarelli G, Cifola I, Grasselli C, Strada G, Bovo G, Perego RA, Bianchi C. 36-kDa Annexin A3 isoform negatively modulates lipid storage in clear cell renal cell carcinoma cells. *Am J Pathol*. 2020;190(11):2317–26.
24. Tang C, Xie AX, Liu EM, Kuo F, Kim M, DiNatale RG, Golkaram M, Chen YB, Gupta S, Motzer RJ, et al. Immunometabolic Coevolution defines unique microenvironmental niches in CcRCC. *Cell Metab*. 2023;35(8):1424–e14401425.
25. Yang G, Cheng J, Xu J, Shen C, Lu X, He C, Huang J, He M, Cheng J, Wang H. Metabolic heterogeneity in clear cell renal cell carcinoma revealed by single-cell RNA sequencing and Spatial transcriptomics. *J Transl Med*. 2024;22(1):210.
26. Zheng M, Zhai Y, Yu Y, Shen J, Chu S, Focaccia E, Tian W, Wang S, Liu X, Yuan X, et al. TNF compromises intestinal bile-acid tolerance dictating colitis progression and limited Infiximab response. *Cell Metab*. 2024;36(9):2086–103. e2089.
27. Li X, Shang S, Wu M, Song Q, Chen D. Gut microbial metabolites in lung cancer development and immunotherapy: novel insights into gut-lung axis. *Cancer Lett*. 2024;598:217096.
28. Sipos A, Ujlaki G, Miko E, Maka E, Szabo J, Uray K, Krasznai Z, Bai P. The role of the Microbiome in ovarian cancer: mechanistic insights into oncobiosis and to bacterial metabolite signaling. *Mol Med*. 2021;27(1):33.
29. Kiss B, Miko E, Sebo E, Toth J, Ujlaki G, Szabo J, Uray K, Bai P, Arkosy P. Oncobiosis and microbial metabolite signaling in pancreatic adenocarcinoma. *Cancers (Basel)*. 2020;12(5).
30. Luu TH, Bard JM, Carbonnelle D, Chaillou C, Huvelin JM, Bobin-Dubigeon C, Nazih H. Lithocholic bile acid inhibits lipogenesis and induces apoptosis in breast cancer cells. *Cell Oncol (Dordr)*. 2018;41(1):13–24.
31. Kovacs P, Csonka T, Kovacs T, Sari Z, Ujlaki G, Sipos A, Karanyi Z, Szeocs D, Hegedus C, Uray K et al. Lithocholic Acid, a Metabolite of the Microbiome, Increases Oxidative Stress in Breast Cancer. *Cancers (Basel)*. 2019;11(9).
32. Li C, Wang L, Xie W, Chen E, Chen Y, Li H, Can D, Lei A, Wang Y, Zhang J. TGR5 deficiency in excitatory neurons ameliorates Alzheimer's pathology by regulating APP processing. *Sci Adv*. 2024;10(26):ead01855.
33. Liu R, Li X, Hylemon PB, Zhou H. Conjugated bile acids promote invasive growth of esophageal adenocarcinoma cells and Cancer stem cell expansion via sphingosine 1-Phosphate receptor 2-Mediated Yes-Associated protein activation. *Am J Pathol*. 2018;188(9):2042–58.
34. Hong J, Behar J, Wands J, Resnick M, Wang LJ, DeLellis RA, Lambeth D, Souza RF, Spechler SJ, Cao W. Role of a novel bile acid receptor TGR5 in the development of oesophageal adenocarcinoma. *Gut*. 2010;59(2):170–80.
35. Wang X, Sun L, Wang X, Kang H, Ma X, Wang M, Lin S, Liu M, Dai C, Dai Z. Acidified bile acids enhance tumor progression and telomerase activity of gastric cancer in mice dependent on c-Myc expression. *Cancer Med*. 2017;6(4):788–97.
36. Ni Z, Min Y, Han C, Yuan T, Lu W, Ashktorab H, Smoot DT, Wu Q, Wu J, Zeng W, et al. TGR5-HNF4alpha axis contributes to bile acid-induced gastric intestinal metaplasia markers expression. *Cell Death Discov*. 2020;6:56.
37. Nguyen PT, Kanno K, Pham QT, Kikuchi Y, Kakimoto M, Kobayashi T, Otani Y, Kishikawa N, Miyauchi M, Arihiro K, et al. Senescent hepatic stellate cells caused by deoxycholic acid modulates malignant behavior of hepatocellular carcinoma. *J Cancer Res Clin Oncol*. 2020;146(12):3255–68.
38. Kainuma M, Takada I, Makishima M, Sano K. Farnesoid X receptor activation enhances transforming growth factor beta-Induced Epithelial-Mesenchymal transition in hepatocellular carcinoma cells. *Int J Mol Sci*. 2018;19(7).
39. Reddy BS, Wynder EL. Metabolic epidemiology of colon cancer. Fecal bile acids and neutral sterols in colon cancer patients and patients with adenomatous polyps. *Cancer*. 1977;39(6):2533–9.
40. Zeng H, Claycombe KJ, Reindl KM. Butyrate and deoxycholic acid play common and distinct roles in HCT116 human colon cell proliferation. *J Nutr Biochem*. 2015;26(10):1022–8.
41. Jin Q, Noel O, Nguyen M, Sam L, Gerhard GS. Bile acids upregulate BRCA1 and downregulate Estrogen receptor 1 gene expression in ovarian cancer cells. *Eur J Cancer Prev*. 2018;27(6):553–6.
42. Fang Y, Qin M, Zheng Q, Wang K, Han X, Yang Q, et al. Role of bile acid receptors in the development and function of diabetic nephropathy. *Kidney Int Rep*. 2024.
43. Xiao H, Sun X, Liu R, Chen Z, Lin Z, Yang Y, Zhang M, Liu P, Quan S, Huang H. Gentipicroside activates the bile acid receptor Gpbar1 (TGR5) to repress NF-kappaB pathway and ameliorate diabetic nephropathy. *Pharmacol Res*. 2020;151:104559.
44. Su J, Zhang Q, Qi H, Wu L, Li Y, Yu D, Huang W, Chen WD, Wang YD. The G-protein-coupled bile acid receptor Gpbar1 (TGR5) protects against renal inflammation and renal cancer cell proliferation and migration through antagonizing NF-kappaB and STAT3 signaling pathways. *Oncotarget*. 2017;8(33):54378–87.
45. Cancer Genome Atlas Research N. Comprehensive molecular characterization of clear cell renal cell carcinoma. *Nature*. 2013;499(7456):43–9.
46. Raufman JP, Chen Y, Zimniak P, Cheng K. Deoxycholic acid conjugates are muscarinic cholinergic receptor antagonists. *Pharmacology*. 2002;65(4):215–21.
47. Li W, Wang X, Zhang X, Gong P, Ding D, Wang N, Wang Z. Revealing potential lipid biomarkers in clear cell renal cell carcinoma using targeted quantitative lipidomics. *Lipids Health Dis*. 2021;20(1):160.

Publisher's note

Springer Nature remains neutral with regard to jurisdictional claims in published maps and institutional affiliations.